Published in final edited form as:
J Bone Miner Res. 2003 September ; 18(9): 1612–1621. doi:10.1359/jbmr.2003.18.9.1612.

A Missense Mutation in the Mouse *Col2a1* Gene Causes Spondyloepiphyseal Dysplasia Congenita, Hearing Loss, and Retinoschisis

LEAH RAE DONAHUE[1,2], **BO CHANG**[1,2], **SUBBURAMAN MOHAN**[3], **NAO MIYAKOSHI**[3], **JON E WERGEDAL**[3], **DAVID J BAYLINK**[3], **NORMAN L HAWES**[1], **CLIFFORD J ROSEN**[1], **PATRICIA WARD-BAILEY**[1], **QING Y ZHENG**[1], **RODERICK T BRONSON**[1], **KENNETH R JOHNSON**[1], and **MURIEL T DAVISSON**[1]

[1]The Jackson Laboratory, Bar Harbor, Maine, USA.

[3]Musculoskeletal Diseases Center, J. L. Pettis VA Medical Center, Loma Linda, California, USA.

Abstract

A missense mutation in the mouse *Col2a1* gene has been discovered, resulting in a mouse phenotype with similarities to human spondyloepiphyseal dysplasia (SED) congenita. In addition, SED patients have been identified with a similar molecular mutation in human *COL2A1*. This mouse model offers a useful tool for molecular and biological studies of bone development and pathology.

Introduction—A new mouse autosomal recessive mutation has been discovered and named spondyloepiphyseal dysplasia congenita (gene symbol *sedc*).

Materials and Methods—Homozygous *sedc* mice can be identified at birth by their small size and shortened trunk. Adults have shortened noses, dysplastic vertebrae, femora, and tibias, plus retinoschisis and hearing loss. The mutation was mapped to Chr15, and *Col2a1* was identified as a candidate gene.

Results—Sequence analyses revealed that the affected gene is *Col2a1*, which has a missense mutation at exon 48 causing an amino acid change of arginine to cysteine at position 1417. Two human patients with spondyloepiphyseal dysplasia (SED) congenita have been reported with the same amino acid substitution at position 789 in the human *COL2A1* gene.

Conclusions—Thus, *sedc/sedc* mice provide a valuable model of human SED congenita with molecular and phenotypic homology. Further biochemical analyses, molecular modeling, and cell culture studies using *sedc/sedc* mice could provide insight into mechanisms of skeletal development dependent on *Col2a1* and its role in fibril formation and cartilage template organization.

Keywords

rodent; chondrocyte; cartilage; collagen; bone density

Address reprint requests to: Leah Rae Donahue, PhD The Jackson Laboratory 600 Main Street Bar Harbor, ME 04609, USA lrd@jax.org.

[2]These authors contributed equally to this article.

The authors have no conflict of interest.

INTRODUCTION

OSTEOCHONDRODYSPLASIAS COMPRISE A LARGE group of conditions that present with a variety of clinical skeletal phenotypes from severe, lethal abnormalities to less severe short stature. More than 100 types of human osteochondrodysplasias have been identified that involve joint abnormalities, impaired growth of long bones, and often have effects in eyes and ears.(1) The chondrodysplasias, a subgroup of the osteochondrodysplasias, have abnormalities in the growth of long bone and spine.(2) The basis for further classification of the chondrodysplasias is the region of long bone most affected; hence subclasses include epiphyseal, metaphyseal, and diaphyseal dysplasias.(2) If the vertebrae are also affected, the subclass for the condition is spondyloepiphyseal dysplasia.(2) Chondrodysplasias are relatively rare in the human population and may appear to be sporadic, or they may have a recognized pattern of inheritance that is dominant or recessive, with autosomal or X-linked transmission.(1) Molecular analyses of gene mutations responsible for these human dysplasias have shown that different mutations in the same gene may result in the same or a slightly different phenotype, and that locus heterogeneity exists, whereby indistinguishable phenotypes are caused by mutations in different genes.(1,3–7) Because a large number of chondrodysplasias have been identified both in humans and mice, the genetic and phenotypic analyses of these disorders continue to provide insight into complex pathways of skeletal development.

At least five different types of collagen-I, II, IX, X, and XI-are associated with cartilage abnormalities in humans and in mice. Among collagens, type II is the most abundant protein in articular cartilage and has been shown to be involved in many forms of chondrodysplasias and the associated cartilage degeneration.(1) The mouse type II collagen gene, *Col2a1*, is highly conserved with its human homolog, *COL2A1*, in exon/intron structure, intron lengths, intronic transcription factor binding sites, and regulatory elements.(8–10) The type II collagen gene in both species encodes the a-chains of type II collagen, a homotrimer of three identical a-chains.(1) Mutations in this gene limit formation of the triple helical assembly of cartilage, and several studies in humans have shown that the severity of the clinical phenotype corresponds to the number of altered collagen fragments left unfolded and to their altered mobility.(11,12) Human patients heterozygous for mutations in the *COL2A1* gene have been diagnosed with many types of skeletal dysplasias including achondrogenesis type II, hypochondrogenesis, spondyloepiphyseal dysplasia congenita, Kniest syndrome, Stickler syndrome, and Wagner syndrome.(13) Each human clinical phenotype has similarities and differences, and each is associated with a different molecular defect in the *COL2A1* gene, including deletions, insertions, splicing mutations, and point mutations.(14,15) *COL2A1* is specifically transcribed in a limited number of human tissues including articular cartilage, the vitreous of the eye, and the nucleus pulposi of the spine, but the specific combination of affected sites coupled with the variability in severity of effect results in a variety of clinical syndromes.(16)

We have discovered a naturally occurring missense mutation in the mouse *Col2a1* gene at exon 48 that results in a cysteine substitution for an arginine. This mouse mutation in the *Col2a1* gene is molecularly similar to that found in the homologous human *COL2A1* gene in two patients with chondrodysplastic features, given the subclassification of spondyloepiphyseal dysplasia congenita (14,15). Mice homozygous for this mutation in *Col2a1* have shortened axial and appendicular skeletons with abnormal growth plates in the vertebrae and long bones, undefined nucleus pulposi, plus retinoschisis, and impaired hearing. Because the mouse phenotype resembles the human clinical phenotype, we have named the new mouse mutant allele spondyloepiphy-seal dysplasia congenita (*sedc*). This new mutation offers a viable and valuable model of human cartilage disease for mechanistic studies.

MATERIALS AND METHODS

Mice

The *sedc* phenotype was discovered in the Mouse Mutant Resource at The Jackson Laboratory in 1997, when a male mouse with spinning behavior was observed. Homozygous *sedc* mice often can be identified at birth by their head bobbing behavior. With age, the bodies of *sedc/sedc* mice are shorter and squarer than normal littermates, and reduced in weight. Both sexes are fertile, and females have normal litter size and number. Genotyping on chromosome (Chr) 15 showed that the *sedc* mutation arose on the C57BL/6J chromosome in a mixed background comprised of C57BL/6J, C3H/HeJ, and AKR/J strains. The *sedc* mutation is currently maintained on the original mixed background by crossing a homozygous male or female to a heterozygote of the opposite sex.

Mice for this work were produced in our colony and maintained under 14:10-h light:dark cycles; autoclaved diet National Institutes of Health-31 (6% fat, 18% protein, Ca:P 1:1, vitamin and mineral fortified; PMI, Richmond, IN, USA) and HCl acidified water (pH 2.8–3.2) were provided ad libitum. Mice were housed in groups of four or five within 51-in^2 polycarbonate boxes on sterilized shavings of Northern White Pine as bedding. Serum was harvested and skeletal preparations were made at necropsy. All procedures were approved by The Jackson Laboratory's Institutional Animal Care and Use Committee and performed in accordance with National Institutes of Health guidelines for the care and use of animals in research.

Mapping of the sedc *mutation*

The *sedc* mutation was mapped in the Mouse Mutant Resource at The Jackson Laboratory using F2 mice from an intercross of F1 hybrids from matings of homozygous *sedc/sedc* mice with mice of the wild-derived strain CAST/Ei. DNA was isolated from frozen spleens of sixty affected F2 mice using phenol/chloroform extraction and typed for polymorphic markers throughout the genome using standard polymerase chain reaction (PCR) methodology.(17) Gene order and recombination frequencies were calculated with the Map Manager computer program.(18) Linkage data for individual F2 mice have been deposited in the Mouse Genome Database, accession number MGD J:68217.

Gene identification/genomic sequencing

To test the *Col2a1* gene as a candidate, we designed four pairs of PCR primers based on mRNA sequence from GenBank accession number M65161 (Table 1). For direct sequencing, the PCR reaction was scaled up to 30 μl; amplification was done during 36 cycles with a 15-s denaturing step at 94°C, a 2-minute annealing step at 60°C, and a 2-minute extension step at 72°C. PCR products were purified from agarose gels using a Qiagen kit (Qiagen Co., Valencia, CA, USA). Sequencing reactions were carried out with automated fluorescence tag sequencing. Genomic DNA was prepared from spleens of 3-week-old mice according to standard procedures. Total RNA was isolated from retinas of newborn mice by TRIZOL LS Reagent (GIBCO BRL, Web Scientific, Crewe, Cheshire, UK) and the SuperScript preamplification system (GIBCO BRL) was used to make first strand cDNA. For *BstF5I* digestion, we designed another pair of primers to amplify genomic DNA to confirm the mutation: Col2a48F 5′-TTGGTCCCTCTGGCAAAG-3′ and Col2a48R 5′-AACAGGGCCTGTTTCTCCTG-3′. Amplification was done during 36 cycles with a 15-s denaturing step at 94°C, a 1-minute annealing step at 51°C, and a 1-minute extension step at 72°C. *BstF5I* digestion was carried out directly in a 10-μl volume by adding 8 μl of PCR products, 1 μl of 10× buffer (SE Buffer 5), and 2–5 U of *BstF5I* (SibEnzyme, Academtown, Russia).

X-rays

Images were obtained using a Faxitron MX20 cabinet X-ray (Faxitron X-Ray Corp., Wheeling, IL, USA) with 1–5× magnification capabilities. Kodak Min-R 2000 mammography film (Eastman Kodak Co., Windsor, CO, USA) was used for maximum resolution.

Morphometrics

The skeletal indices (length, height, width) of the right femur, right tibia, and L6 vertebrae were measured with a dial caliper (Mitutoyo, Kanagawa, Japan) to 0.01 mm. Craniofacial measurements were taken with a digital caliper (Stoelting, Wood Dale, IL, USA) from skulls prepared by incomplete maceration in potassium hydroxide, stained with alizarin red, and stored in undiluted glycerin.(19)

Histology and dynamic histomorphometry

Mutant and control mice at 4 months and 1 year of age were deeply anesthetized with tribromoethanol and killed by intracardial perfusion of Bouin's fixative following flushing of the vasculature with physiological saline. Longitudinal and cross-sections of the lumbar spine (L2–L5) and distal femur were stained with hematoxylin and eosin (H&E). For the evaluation of the femoral growth plate, femurs from 2- and 6-week-old mice were decalcified in 14% EDTA solution for 10 days at 4°C and embedded in paraffin. Five-micrometer-thick sections in the mid-frontal plane were obtained and were stained with toluidine blue.

For dynamic histomorphometry, 6- to 16-week-old mice (5–11 per group) were labeled with tetracycline (20 mg/kg) and then declomycine (20 mg/kg) with a 6-day interval. Tissues were harvested 1 day after the declomycine label. The calvaria, lumbar spine, and both femora and tibias were removed and fixed with 10% cold neutral buffered formalin. All histomorphometric parameters were measured with the OsteoMeasure system equipped with a digitizing tablet (OsteoMetrics, Atlanta, GA, USA) and a color video camera (Sony, Tokyo, Japan). Measurements were made at a total magnification of ×600 (×20 microscope objective and ×30 camera magnification). The cancellous bone area (tissue volume [TV]) at secondary spongiosa was measured in a standardized sampling site 250 μm distal to the growth plate-metaphyseal junction to exclude primary spongiosa.

Nomenclature and symbols used in bone histomorphometry are the same as those described in the report of the American Society for Bone and Mineral Research Committee.(20) The following histomorphometric parameters were measured: longitudinal growth rate (LGR, μm/day), the distance between the fluorescent labels at the metaphysis divided by the fluorescent period; percent cancellous bone volume (BV/TV, %), the percentage of cancellous bone volume to TV; trabecular thickness (Tb.Th, μm), the BV/TV divided by one-half the bone surface (BS); percent osteoid surface (OS/BS, %), the percentage osteoid surface to BS; mineral apposition rate (MAR, μm/day), the mean of the width of the double labels divided by the interlabel time; volume referent bone formation rate (BFR/TV,%/year), MAR × (1/2 × single-labeled surface + double-labeled surface)/TV × 365 × 100%; percent eroded surface (ES/BS, %), percentage eroded surface to BS; percent osteoclast surface (Oc.S/BS, %), percentage osteoclast surface to BS; and osteoclast number (N.Oc/TV, /mm^2). We identified osteoclasts as multinucleated cells on eroded surfaces.

Assessment of hearing

Hearing was assessed by auditory-evoked brainstem response (ABR) thresholds with equipment from Intelligent Hearing Systems (HIS, Miami, FL, USA) using previously described methods and equipment.(21) Subdermal needle electrodes are inserted at the vertex and ventrolaterally to both ears of anesthetized mice. Specific auditory stimuli (broad-band

click and pure-tone pips of 8, 16, and 32 kHz) from high-frequency transducers are delivered binaurally through plastic tubes to the ear canals. Evoked brainstem responses are amplified and averaged, and their wave patterns displayed on a computer screen. Auditory thresholds are obtained for each stimulus by varying the sound pressure level (SPL) to identify the lowest level at which an ABR pattern can be recognized.

Statistical analysis

Data are presented as means ± SE. Statistical analyses were performed with StatView 4.5 (Abacus Concepts, Berkeley, CA, USA) software for Macintosh. Results for each measured parameter were analyzed by three-way ANOVA with gender, time, and genotype as the variables. Results were considered significantly different at $p < 0.05$.

RESULTS

sedc *maps to Chr 15 and is a mutation of* Col2a1

The *sedc* mutation was mapped to mouse Chr15 between *D15Mit74* and *D15Mit44* in a region homologous with human Chr 12q12–13; no recombination between *sedc* and *D15Mit41*was detected in 60 *sedc/sedc* mice. Because homozygotes exhibited a skeletal phenotype consistent with a collagen mutation (see below), and because *D15Mit41* is within the *Col2a1* gene,(22) we determined *Col2a* to be a likely candidate gene.

Sequence analysis of the *Col2a1* gene showed that the *sedc/sedc* mutation is caused by a missense mutation in exon 48 that changes codon 1417 CGC to TGC, resulting in an arginine to a cysteine (Arg1417Cys) change (Fig. 1). This mutation resulted in the creation of a new *BstF5I* restriction site (Fig. 1) that enabled us to genotype the *sedc* mutation by PCR/restriction fragment length polymorphism (RFLP). To confirm the presence of the missense codon in the *sedc Col2a1* gene, we re-examined 46 DNAs (15 affected and 31 unaffected mice) from our linkage analysis for the *BstF5I* RFLP. We amplified a Col2a48F/Col2a48R 92-bp genomic fragment that contains one *BstF5I* site in the *sedc* allele and none in the normal allele (Fig. 1). Digestion of the PCR amplified products with *BstF5I* from wild-type, heterozygous, and homozygous *sedc* DNA revealed the predicted RFLP pattern (wild-type—one band of 92 bp; heterozygous *sedc*—three bands of 92, 72, and 20 bp; homozygous *sedc*—two bands of 72 and 20 bp). This analysis showed that there was absolute concordance between the *sedc/sedc* phenotype and the missense mutation ($\chi 2 = 46$, $p < 0.001$). The RFLP pattern thus provides a tool for verification of the presence or absence of the *sedc* allele in genetic analyses.

To determine whether the sequence alteration at codon 1417 was specific for the *Col2a1* gene of the *sedc/sedc* mice, we analyzed the corresponding genomic DNA region in 12 different inbred mouse strains by RFLP analysis and found that none of the 12 had the *BstF5I* site present. BLAST results from the nuclear acid database for nucleotide C at position 4249 or from the protein database for amino acid R at position 1417 of the *Col2a1* gene indicated that the nucleotide C or amino acid R is conserved across all species examined including *Mus musculus*, *Rattus norvegicus*, *Homo sapiens*, *Equus caballus*, *Canis familiaris*, *Gallus gallus*, *Gallus gallus*, *Oryctolagus cuniculus*, *Danio rerio*, and *Cynops pyrrhogaster*. These results further argue that the C to T transition at position 4249 of the *Col2a1* gene is the mutation underlying *sedc* rather than a sequence polymorphism. The gene symbol for the *sedc* mutation has subsequently been assigned $Col2a1^{sedc}$.

Skeletal abnormalities detected by X-rays and morphometrics

Visual examination of *sedc/sedc* mice showed shortening of the trunk and long bones. Body weight of *sedc/sedc* males and females compared with unaffected controls was reduced by approximately 20% at 4 weeks of age and by 30% at 8, 12, and 16 weeks of age. Tail length

was reduced by approximately12% in both male and female *sedc/sedc* mice at 4, 8, 12, and 16 weeks compared with gender-matched unaffected mice, and back length in *sedc/sedc* males and females was reduced by an average of 14% from 4 to 16 weeks of age. Radiographic examination at ×3 and ×5 magnification showed that the thoracic and lumbar vertebral bodies of *sedc/sedc* mice were shorter and wider than those of unaffected (*sedc*/+) littermates (Fig. 2). Skeletal indices of vertebra and long bones (Fig. 3) showed that bones of *sedc/sedc* mice were significantly shorter but wider than controls (Table 2). In addition, *sedc/sedc* mice had shortened skulls, whereas height and width of the skull were unaffected. Measurements of nine *sedc/sedc* mice and six controls demonstrated that the skull length in affected mice was reduced by 5%; upper jaw length was reduced by 4%; and lower jaw length was reduced by 10%, compared with controls.

Abnormal growth plates by histology and dynamic histomorphometry

Longitudinal sections of the spine and spinal cord were prepared from *sedc/sedc* and control mice at 4, 8, and 16 weeks of age, and similar histological pathology was seen at all ages. The intervertebral disc cartilage in heterozygous control mice was well organized into annulus fibrosus and nucleus pulposus as shown at 16 weeks (Fig. 4A). A comparable section from a 16-week-old *sedc/sedc* mouse (Fig. 4B) showed shorter and wider vertebral bodies. The end plates of the vertebral bodies were splayed and irregular with no defined growth plate. In addition, the intervertebral disc cartilage was disorganized in mice at all ages examined, and the border between annulus fibrosus and nucleus pulposus of the disc was unclear. A dramatic example of the increased size of the central vertebral body is shown in Fig. 4D. This cross-section of L5 was taken from a 1-year-old *sedc/sedc* female with severe protrusion of the proliferative cartilage in the dorsal vertebral body, causing compression of the spinal cord. A cross-section of L5 from a normal mouse is shown in Fig. 4C for comparison.

Longitudinal sections of the distal femur from 16-week-old *sedc/sedc* and control mice are shown in Figs. 5A and 5B. Comparison of the *sedc/sedc* to the control showed an enlarged and disorganized growth plate with irregularly thickened articular cartilage. A similar section from a 1-year-old affected mouse is shown in Fig. 5C and exhibits the degeneration of articular cartilage often seen in older *sedc/sedc* mice, whereby the superficial layers of the articular cartilage separate from the deeper layers. Although we cannot explain why the overgrowth of the vertebral body is greater than enlargement of the growth plate in the femur, in our studies of mice, it is not uncommon to find that the skeletal response to environmental and genetic influences varies from one bone site to another.

Mid-frontal sections of the proximal growth plate of the femur from 2- and 6-week-old *sedc/sedc* and control mice are shown in Figs. 6A–6D. Mutant mice showed an absence of the typical columnar arrangement of cells with a reduction in the number of proliferating and hypertrophic chondrocytes (Figs. 6B and 6D). These observations were more evident in 6-week-old mice (Fig. 6D) than in younger mice (Fig. 6B). However, no reduction of the height of growth plate cartilage was seen at any age in affected mice. The distribution of primary spongiosa in *sedc/sedc* mice was slightly irregular and shorter than in control mice. However, $TRACP^{+}$ osteoclasts in the zone of resorption were uniformly distributed both in the *sedc/sedc* and control mice (data not shown). Invasion of blood vessels into empty lacunae showed no distinct differences between the groups. There was no noticeable difference in intramembranous bone formation in calvaria examined by H&E- and toluidine blue–stained sections between affected mice and controls (data not shown).

Histomorphological parameters of longitudinal growth rate, bone formation rate, and bone resorption rate measured in this study all significantly decreased with age in both *sedc/sedc* and normal mice, while there was no significant effect of age on bone volume or trabecular thickness in either *sedc/sedc* or control mice (Table 3). Consistent with the reduced longitudinal

bone growth in *sedc/sedc* mice, as determined by femur and back length, the longitudinal growth rate in mutant mice was significantly less than in control animals by an average of 38% at each age examined. Bone volume and trabecular thickness in *sedc/sedc* mice were significantly less (17% and 15%, respectively). Osteoid volume, mineral apposition rate, bone formation rate, and osteoclast number in the *sedc/sedc* mice were significantly less by an average of 33%, 15%, 30%, and 32%, respectively. Eroded and osteoclast surface were not significantly different between *sedc/sedc* and control groups.

Impaired hearing and retinoschisis

Mice homozygous for the *sedc* mutation exhibit head bobbing and circling behavior. Such balance defects indicate vestibular dysfunction of the inner ear, which often is associated with cochlear dysfunction. Therefore, we assessed hearing in these mice by auditory brainstem response (ABR) threshold analysis. At 10–15 weeks of age, 1 of the 12 *sedc/sedc* mice tested was completely deaf, failing to respond to the most intense auditory stimuli presented. All of the remaining 11 *sedc/sedc* mice exhibited significant hearing impairment, with ABR thresholds 35–50 dB above +/+ mice from the progenitor strains. No abnormalities were apparent at the light microscopic level in whole mounts and cross sections of inner ears from *sedc/sedc* mice; consequently, the head bobbing behavior remains unexplained.

Examination of eyes from mutant mice revealed that most had an unusual retinal lesion. Portions of the inner nuclear layer (INL) had split apart such that clefts formed between the inner and outer aspects of the INL. This finding was quite distinct from the common artifact of retinal detachment in which clefts appear between the photoreceptor layer and the pigment epithelial layer. The INL clefts varied in size and location from mouse to mouse in *sedc/sedc* mutants, and sections of eyes of some mutants had no retinal lesions. The lesion was never observed in control mice. Clefting within the INL occurs in humans and is called retinoschisis. A more comprehensive description of this lesion will be published elsewhere.

DISCUSSION

At least 20 mutations have been identified in the human gene encoding type II collagen,(1) each resulting in a somewhat different clinical phenotype. Linkage studies have identified patients with chondrodysplasias of one variety or other that are associated with each of these mutations, including both missense and nonsense types.(12,14,23–25) The correlation between each type of mutation or the site of the mutation and the clinical phenotype are not well understood.(1,13,14) Genetic analyses have shown that different mutations in the same gene may result in the same clinical phenotype, or a slightly different phenotype, and that locus heterogeneity exists, whereby clinically indistinguishable phenotypes are caused by mutations in different genes.(26,27) A possible explanation for locus heterogeneity is that many of the genes responsible for the formation of cartilage code for molecules with multiple domains involved in different interactions and participating in the formation of multimeric structural complexes or multistep signaling pathways.(28) Thus, genetic and phenotypic analyses of the large variety of chondrodysplasias identified in both humans and mice provide insight into the complex pathways of skeletal development.(29,30)

We have described here a new mutation in the mouse that is analogous to the mutation in the human *COL2A1* gene responsible for spondyloepipyseal dysplasia (SED) congenita in two human patients reported to date.(14,15) In the *sedc* mouse, there is a missense mutation in exon 48 that changes codon 1417 CGC to TGC, causing an arginine to a cysteine change in the COL2A1 protein. In the two human patients with relatively severe SED congenita, the arginine to cysteine substitution occurs at position 789.(14,15) The substitution of a cysteine for an arginine in the Y-position of the Gly-X-Y triplet is of special interest because cysteine is not normally found in the triple-helical domain of type II collagen in any species.(13) A cysteine

at this position provides the opportunity for disulfide bonds to form, thus disrupting the formation of collagen fibrils.(31,32) In humans, three arginine to cysteine mutations in the *COL2A1* gene have been found at positions 75, 519, and 789, with SED varying in severity; all three mutations have been found in more than one unrelated individual.(13) The *sedc* mouse model shares not only unique molecular similarity with human SED but also the most common clinical phenotypes including abnormal epiphyses, flattened vertebral bodies, and involvement of the eyes and ears. As in the human, defects in the *sedc* mouse skeleton are specific to tissues with type II collagen, that is, endochondral bone, whereas intramembranous bone is normal. The eye phenotype, however, differs between human SED patients and the *sedc* mouse. Whereas SED patients often have myopia with vitreal degeneration and retinal detachment, (12,25) *sedc* mice have retinoschisis, characterized by clefts between the inner and outer aspects of the inner nuclear layer. Both human SED congenita patients(33) and *sedc* mice suffer hearing loss.

Recently, a transgenic mouse model was constructed using a type II collagen transgene with an arginine to cysteine switch at position 789 and a murine *Col2a1* promoter directing the gene expression to cartilage.(34) Mice carrying the transgene were shorter overall, had shorter limbs with disorganized growth plates, a short nose, cleft palate, and died at birth. Using cell culture experiments and molecular modeling Gaiser et al.(34) suggested that this Y-position mutation acts in a dominant negative way resulting in destabilization of collagen molecules during assembly, reduction in the number of fibrils formed, and abnormal cartilage template function. Although our recessive naturally occurring *sedc* mutation is molecularly similar, the resulting phenotype is much less severe, whereby mice survive to adulthood and reproduce normally. It is possible that the endogenous COL2A1 protein in the transgenic mouse is overwhelmed by the quantity of abnormal COL2A1 induced by the transgene, resulting in a dominant-negative effect and a more severe phenotype. It is also possible that the insertion site of the transgene has disrupted an additional gene causing a change in the transgenic phenotype. The naturally occurring mutation in *sedc* mice is likely to be more similar to the mutation in human SED congenita patients because both involve only one gene; thus, *sedc* mice offer a better tool to further investigate the unique function of the arginine to cysteine substitution in this Y-position than does the transgenic model.

Other mouse models with mutations in the type II collagen gene have been studied, including numerous transgenics(35–38) and one other naturally occurring mutation, disproportionate micromelia (*Dmm*).(39) The resulting phenotypes in all of the highly expressing transgenic mice, each somewhat different depending on the transgene construct, include an assortment of features associated with human chondrodysplasias-short limbs, disproportionately short stature, small jaw, cleft palate, small thorax, and distended abdomen. All homozygotes were neonatal or perinatal lethal, some because of the inability to breathe.(35,37,40) One transgenic line expressing at low levels developed age-related joint abnormalities that were similar to human osteoarthrosis.(41,42) Transgenic lines were also constructed to overexpress the normal type II collagen gene.(43) In highly expressing lines, thick bundles of collagen fibrils were seen in the growth plate, suggesting that proper assembly of cartilage collagen is dependent on appropriate production of type II collagen. In humans, an example of underproduction of type II collagen is the Stickler syndrome wherein mutations of the human *COL2A1* gene results in null alleles.(25)

The opportunity to study chondrodysplasias in humans is limited because of the high number of mutations found in the *COL2A1* gene and the variability in the clinical phenotype. Variation in the phenotypic expression of the same mutation in different individuals suggests that other genetic and environmental effects play a part in the final clinical expression. These quantitative and epigenetic effects are difficult to understand in the heterozygous human population. Additionally, different mutations in the *COL2A1* gene may result in slightly different clinical

presentations, complicating molecular diagnosis. Animal models can help to interpret the clinical phenomena. The *sedc* mutant strain represents a unique opportunity to study the physiological consequence of a particular *Col2a1* mutation in an infinite number of genetically identical individuals. In addition, this viable model of SED congenita allows testing of new treatment modalities for skeletal dysplasias and offers the potential for experimental gene therapy.

Acknowledgments

We thank Coleen Marden for her help in maintaining our colony of *sedc* mice; Joiel Buschatz for her characterization of the craniofacial abnormalities, and Jennifer Smith for her help in preparing the graphics for this paper. We also thank Drs Wesley Beamer and Patsy Nishina for their careful review of this manuscript. This study was supported by National Institutes of Health Grants RR01183, CA34186, EY07758, DE13078, and AG19698 (SM).

REFERENCES

1. Vikkula M, Metsaranta M, Ala-Kokko L. Type II collagen mutations in rare and common cartilate diseases. Ann Med 1994;26:107–114. [PubMed: 8024727]
2. Whyte, MP. Chondrodystrophies and mucopolysaccharidoses.. In: Favus, MJ., editor. Primer on the Metabolic Bone Diseases and Disorders of Mineral Metabolism. 4th ed.. Lippincott Williams & Wilkins; Philadelphia, PA, USA: 1999. p. 289-393.
3. Francomono C, Liberfarb R, Hirose T, Maumenee I, Streeten E, Meyers D, Pyeritz R. The Stickler syndrome: Evidence for close linkage to the structural gene for type II collagen. Genomics 1987;1:293–296. [PubMed: 2896625]
4. Knowlton RG, Weaer EJ, Struyk AF, Knobloch WH, King RA, Norris K, Shamban A, Uitto J, Jimenez SA, Prockop DJ. Genetic linkage analysis of hereditary arthro-ophthalmopathy (Stickler syndrome) and the type II procollagen gene. Am J Hum Genet 1898;45:681–688. [PubMed: 2573273]
5. Anderson I, Goldberg R, Marion R, Upholt W, Tsipouras P. Spondyloepiphyseal dysplasia congenita: Genetic linkage to type II collagen (COL2A1). Am J Hum Genet 1990;46:896–901. [PubMed: 1971141]
6. Anderson I, Tsipouras P, Schr C, Ramesar R, Martell R, Beighton P. Spondyloepiphyseal dysplasia, mild autosomal dominant type is not due to primary defects of type II collagen. Am J Hum Genet 1990;37:272–276.
7. Sher C, Ramesar R, Martell R, Learmonth I, Tsipouras P, Beighton P. Mild spondyloepiphyseal dysplasia (Namaqualand type): Genetic linkage to the type II collagen gene (COL2A1). Am J Hum Genet 1991;48:518–524. [PubMed: 1671807]
8. Cheah K, Au P, Lau E, Little P, Stubbs L. The mouse Col2a-1 gene is highly conserved and is linked to Int-1 on chromosome 15. Mamm Genome 1991;1:171–183. [PubMed: 1797232]
9. Ala-Kokko L, Kvist A, Metsaranta M, Kivirikko K, de Crombrugghe B, Prockop D, Vuorio E. Conservation of the sizes of 53 introns and over 100 intronic sequences for the binding of common transcription factors in the human and mouse genes for type II procollagen (COL2A1). Biochem J 1995;308:923–929. [PubMed: 8948452]
10. Vikkula M, Metsaranta M, Syvanen A, Ala-Kokko L, Vuorio E, Peltonen L. Structural analysis of the regulatory elements of the type-II procollagen gene. Conservation of promoter and first intron sequences between human and mouse. Biochem J 1992;285:287–294. [PubMed: 1637314]
11. Murray L, Bautista J, James P, Rimoin D. Type II collagen defects in the chondrodysplasias. I. Spondyloepiphyseal dysplasias. Am J Hum Genet 1989;45:5–15. [PubMed: 2741952]
12. Tiller G, Rimoin D, Murray L, Cohn D. Tandem duplication within a type II collagen gene (COL2A1) exon in an individual with spondyloepiphyseal dysplasia. Proc Natl Acad Sci USA 1990;87:3889–3893. [PubMed: 2339128]
13. Kuivaniemi H, Tromp G, Prockop DJ. Mutations in fibrillar collagens (types I. II, III, and XI), fibril-associated collagen (type IX), and network-forming collagen (type X) cause a spectrum of diseases of bone, cartilage, and blood vessels. Hum Mutat 1997;9:300–315. [PubMed: 9101290]

14. Chan D, Taylor TKF, Cole WG. Characterization of an arginine 789 to cysteine substitution in a1(II) collagen chains of a patient with spondyloepiphyseal dysplasia. J Biol Chem 1993;268:15238–15245. [PubMed: 8325895]
15. Chan D, Rogers JF, Bateman JF, Cole WG. Recurrent substitutions of arginine 789 by cysteine in pro-a1 (II) collagen chains produce spondyloepiphyseal dysplasia congenita. J Rheumatol 1995;43 (Suppl):37–38.
16. Miller E, Gay S. The collagens: An overview and update. Methods Enzymol 1987;144:3–41. [PubMed: 3306286]
17. Ward-Bailey PF, Johnson KR, Handel MA, Harris BS, Davisson MT. A new mouse mutation causing male sterility and histoincompatibility. Mamm Genome 1996;7:793–797. [PubMed: 8875885]
18. Manly KF. A Macintosh program for storage and analysis of experimental genetic mapping data. Mamm Genome 1993;4:303–313. [PubMed: 8318734]
19. Green MC. A rapid method for clearing and staining specimens for the demonstration of bone. Ohio J Sci 1952;52:31–33.
20. Parfitt AM, Drezner MK, Glorieux FH, Kanis JA, Malluche H, Meunier PJ, Ott SM, Recker RR. Bone histomorphometry: Standardization of nomenclature, symbols and units. J Bone Miner Res 1987;2:595–610. [PubMed: 3455637]
21. Zheng Q, Johnson K, Erway L. Assessment of hearing in 80 inbred strains of mice by ABR threshold analyses. Hear Res 1999;130:94–107. [PubMed: 10320101]
22. Mouse Genome Informatics Project TJL. Bar Harbor, ME. Mouse Genome Database (MGD). 2002 [February 22, 2001]. Available online at http://www.informatics.jax.org/.
23. Lee B, Vissing H, Ramirez F, Rogers D, Rimoin D. Identification of the molecular defect in a family with spondyloepiphyseal dysplasis. Science 1989;244:978–980. [PubMed: 2543071]
24. Ala-Kokko L, Baldwin C, Moskowitz R, Prockop D. Single base mutation in the type II procollagen gene (COL2A1) as a cause of primary osteoarthritis associated with a mild chondrodysplasia. Proc Natl Acad Sci USA 1990;87:6565–6568. [PubMed: 1975693]
25. Ahmad NN, Ala-Kokko L, Knowlton RG, Jimenez SA, Weaver EJ, Maguire JI, Tasman W, Prockop DJ. Stop codon in the procollagen II gene (COL2A1) in a family with the Stickler syndrome (arthro-ophthalmopathy). Proc Natl Acad Sci USA 1991;88:6624–6627. [PubMed: 1677770]
26. Francomano C, Rowan B, Liberfarb R, Hirose T, Maumene I, Stoll H, Pyeritz R. The Stickler and Wagner syndromes: Evidence for genetic heterogeneity. Am J Hum Genet 1988;43:A218.
27. Schwartz R, Watkins D, Fryer A, Goldberg R, Marion R, Polomeno R, Spallone A, Upadhyayam M, Harper R, Tsipouras P. Non-allelic genetic heterogeneity in the vitreoretinal degenerations of the Stickler and Wagner types and evidence for intagenic recombination at the COL2A1 locus. Am J Hum Genet 1989;45:A218.
28. Pace JM, Li Y, Seegmiller RE, Teuscher C, Taylor BA, Olsen BR. Disproportionate micromelia (Dmn) in mice caused by a mutation in the c-propeptide coding region of col2a1. Dev Dyn 1997;208:25–33. [PubMed: 8989518]
29. Whyte, MP. Chondrodystrophics and mucopolysaccharidoses.. In: Favas, MJ., editor. Primer on the Metabolic Bone Diseases and Disorders of Mineral Metabolism. 4th ed.. Lippincott Williams and Wilkins; Philadelphia, PA, USA: 1999. p. 389-393.
30. Bilezikian, JP.; Raisz, LG.; Rodan, GA., editors. Principles of Bone Biology. 2nd ed.. Vol. 1. Academic Press; San Diego, CA, USA: 2002.
31. Fertala A, Ala-Kokko L, Wiaderkiewicz R, Prockop DJ. Collagen II containing a Cys substitution for arg-alpha1–519 Homotrimeric monomers containing the mutation do not assemble into fibrils but alter the self-assembly of the normal protein. J Biol Chem 1997;272:6457–6464. [PubMed: 9045670]
32. Adachi E, Katsumata O, Yamashina S, Prockop DJ, Fertala A. Collagen II containing a Cys substitution for Arg-alpha1–519 analysis by atomic force microscopy demonstrates that mutated monomers alter the topography of the surface of collagen II fibrils. Matrix Biol 1999;18:189–196. [PubMed: 10372559]
33. McKusick-Nathans Institute for Genetic Medicine JHUB, MDNational Center for Biotechnology Information, National Library of Medicine (Bethesda, MD)2000Available online at

http://www.ncbi.nlm.nih.gov/omim/.January 16, 2001 Online Mendelian Inheritance in Man, OMIM (TM).

34. Gaiser KG, Maddox BK, Bann JG, Boswell BA, Keene DR, Garofalo S, Horton WA. Y-position collagen II mutation disrupts cartilage formation and skeletal development in a transgenic mouse model of spondyloepiphyseal dysplasia. J Bone Miner Res 2002;17:39–47. [PubMed: 11771668]
35. Garofalo S, Vuorio E, Metsaranta M, Rosati R, Toman D, Vaughan J, Lozano G, Mayne R, Ellard J, Horton W, DeCrombrugghe B. Reduced amounts of cartilage collagen fibrils and growth plate anomalies in transgenic mice harboring a glycine-to-cysteine mutation in the mouse type II procollagen alpha 1-chain gene. Proc Natl Acad Sci USA 1991;88:9648–9652. [PubMed: 1946380]
36. Maddox BK, Garofalo S, Smith C, Keene DR, Horton WA. Skeletal development in transgenic mice expressing a mutation at Gly574Ser of type II collagen. Dev Dyn 1997;208:170–177. [PubMed: 9022054]
37. Metsaranta M, Garofalo S, Decker G, Rintala M, DeCrombrugghe B, Vuorio E. Chondrodysplasia in transgenic mice harboring a 15-amino acid deletion in the triple helical domain of pro alpha 1(II) collagen chain. J Cell Biol 1992;118:203–212. [PubMed: 1618904]
38. Vandenberg P, Khillan JS, Prockop DJ, Helminen H, Kontusaari S, Ala-Kokko L. Expression of a partially deleted gene of human type II porcollagen (COL2A1) in transgenic mice produces a chondrodysplasia. Proc Natl Acad Sci USA 1991;88:7640–7644. [PubMed: 1881905]
39. Foster M, Caldwell A, Staheli J, Smith D, Gardner J, Seegmiller R. Pulmonary hypoplasia associated with reduced thoracic space in mice with disproportionate micromelia (DMM). Anat Rec 1994;238:454–462. [PubMed: 8192242]
40. Li SW, Prockop DJ, Helminen H, Fassler R, Lapvetelainen T, Kiraly K, Peltarri A, Arokoski J, Lui H, Arita M, Khillan JS. Transgenic mice with targeted inactivation of the Col2 alpha 1 gene for collagen II develop a skeleton with membranous and perisoteal bone but no endochondral bone. Genes Dev 1995;15:2821–2830. [PubMed: 7590256]
41. Helminen HJ, Kiraly K, Pelttari A, Tammi MI, Vandenberg P, Pereira R, Dhulipala R, Khillan JS, Ala-Kokko L, Hume EL, Sokolov BP, Prockop DJ. An inbred line of transgenic mice expressing an internally deleted gene for type II procollagen (COL2A1). Young mice have a variable phenotype of a chondrodysplasia and older mice have osteoarthritic changes in joints. J Clin Invest 1993;92:582–595. [PubMed: 8349798]
42. Eyre DR, Weis MA, Moskowitz RW. Cartilage expression of a type II collagen mutation in an inherited form of osteoarthritis associated with a mild chondrodysplasia. J Clin Invest 1991;87:357–361. [PubMed: 1985108]
43. Garofalo S, Metsaranta M, Ellard J, Smith C, Horton W, Vuorio E, de Crombrugghe B. Assembly of cartilage collagen fibrils is distrupted by overexpression of normal type II collagen in transgenic mice. Proc Natl Acad Sci USA 1993;90:3825–3829. [PubMed: 8483900]

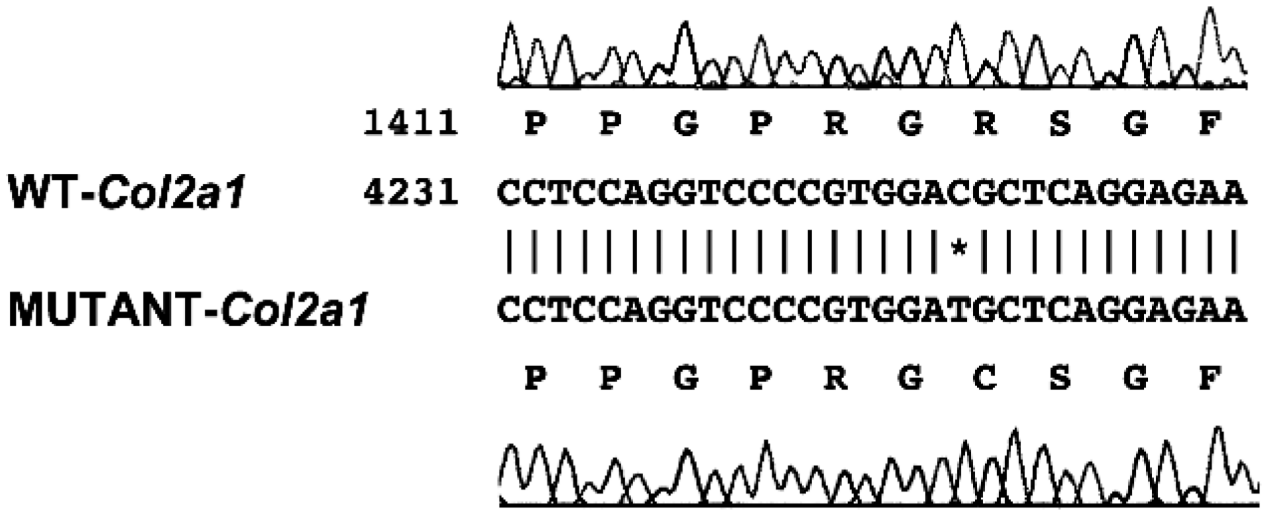

FIG. 1.

Comparison of the nucleotide sequences in exon 48 of the *Col2a1* gene around position 4249, where a single base substitution from C to T is shown for the *sedc* allele. This novel mutation changes codon 1417 CGC to TGC and results in an amino acid change of Arg1417 to Cys in the *Col2a* protein in *sedc/sedc* mice. A *BstF5I* restriction enzyme site GGATG in the *sedc-Col2a1* sequence is also indicated (*).

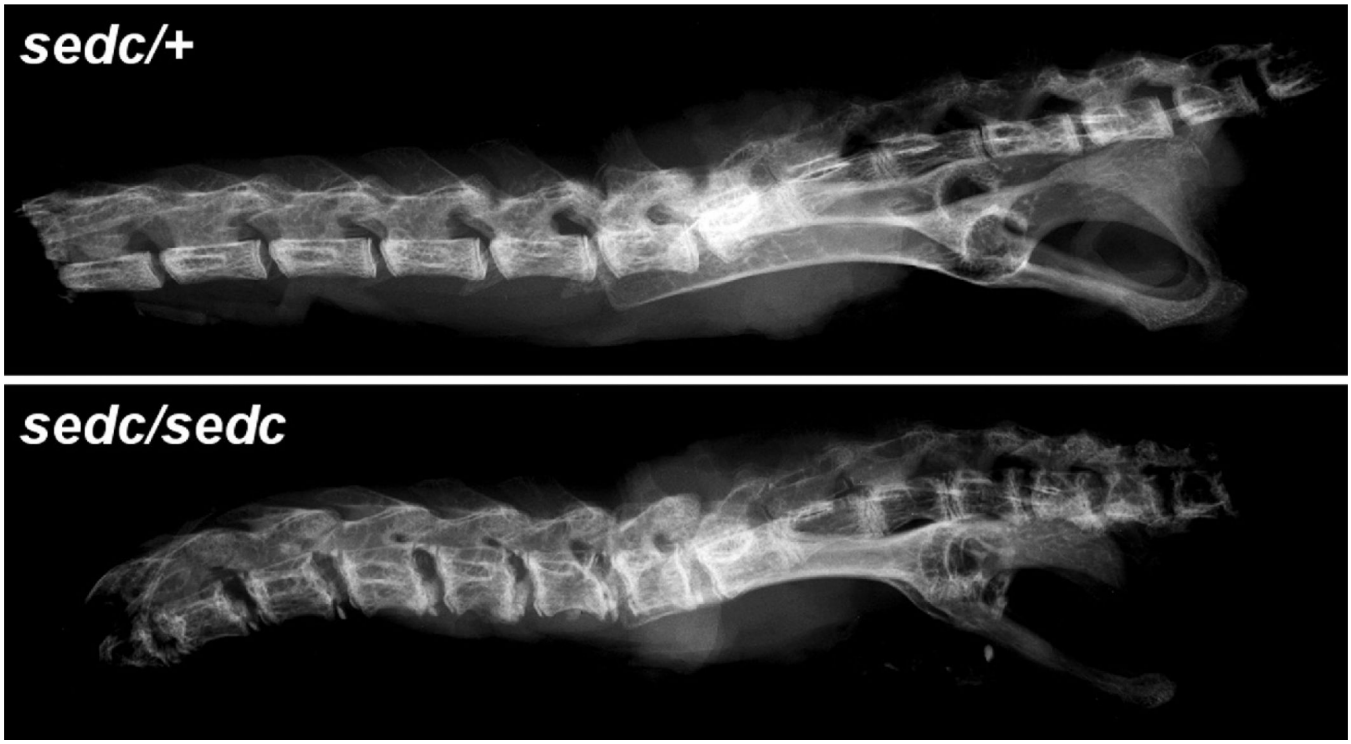

FIG. 2.
Comparison of the thoracic and lumbar vertebrae of 16-week-old heterozygous (*sedc*/+) and homozygous (*sedc/sedc*) mice (magnification ×5). Vertebral bodies are shorter and wider in the *sedc/sedc* spine throughout both thoracic and lumbar regions, with increased mineralization.

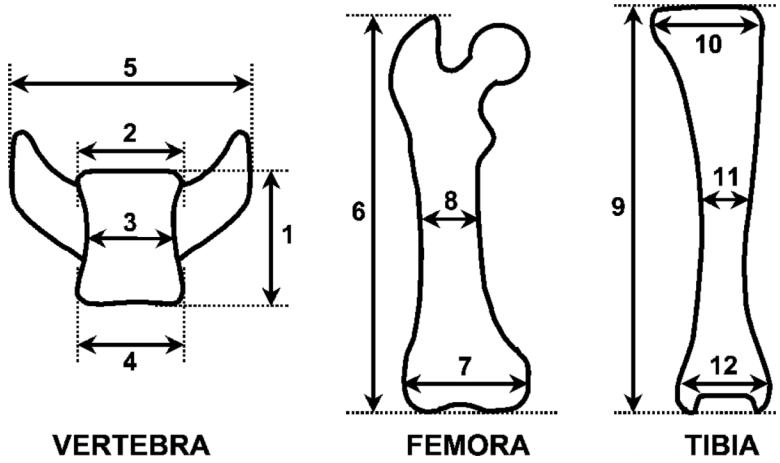

FIG. 3.

Bone parameters in *sedc/sedc* mice.1, vertebral height; 2, upper vertebral width; 3, middle vertebral width; 4, lower vertebral width; 5, transverse processes width; 6, femoral length; 7, femoral condylar width; 8, femoral midshaft width; 9, tibial length; 10, tibial condylar width; 11, tibial midshaft width; and 12, tibial malleolar width.

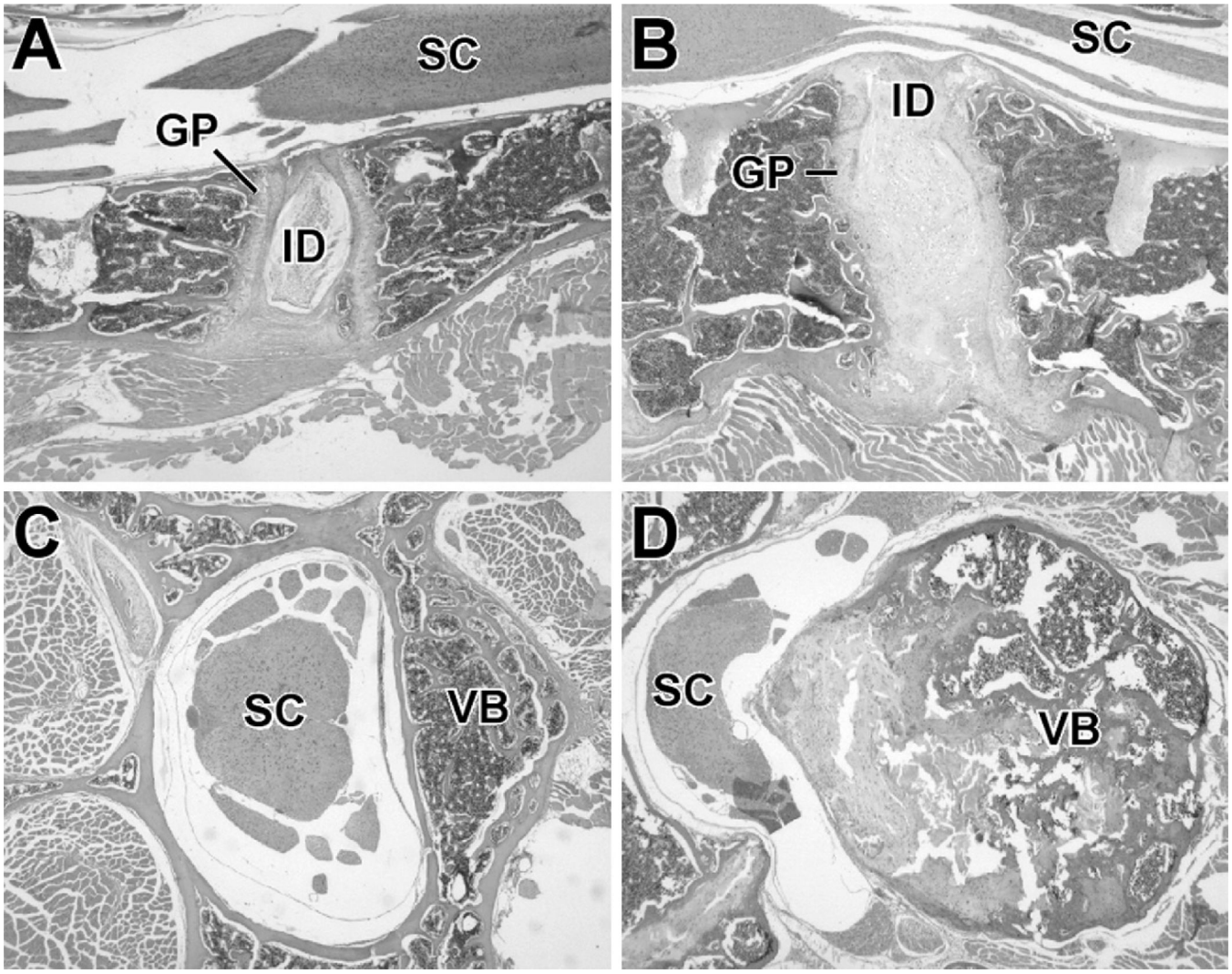

FIG. 4.

(A–D) Histological sections stained with hematoxylin and eosin (H&E) of lumbar vertebrae from *sedc/sedc* and normal mice (magnification ×45). (A) Longitudinal section of spine and spinal cord from a 16-week-old normal mouse. Note the well-defined intervertebral disk (ID) in the center and the relatively straight growth plates (GP) to either side of it. The lumbar spinal cord (SC) is at the top of the section. (B) Comparable section from a 16-week-old *sedc/sedc* mouse. The entire spine is two to three times thicker than the control spine (A). The ID is enlarged and blends with the GPs on either side. The plates are irregularly thickened and project ventrally and dorsally. (C) Cross-section from the spinal cord and spine from a 4-month-old normal mouse. Note the vertebral body (VB) right of the lumbar spinal cord (SC). (D) Cross-section from the spinal cord and spine from a 1-year-old *sedc/sedc* mouse. The vertebral body (VB) is three times larger in diameter than in the normal mouse. Both mature bone and proliferative cartilage contribute to the enlargement. Note that the proliferative cartilage, which is also undergoing degeneration, projects into and deforms the spinal cord (SC).

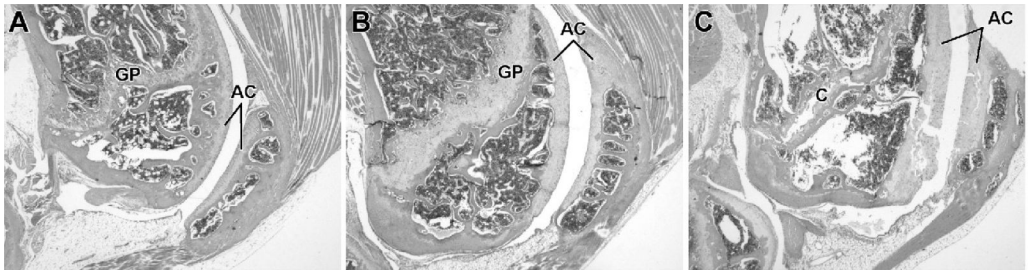

FIG. 5.

(A–C) Histological sections stained with H&E of distal femur and knee from *sedc/sedc* and normal mice (magnification, ×35). (A) Longitudinal section of the distal femur, knee joint, and patella from a 4-month-old control. The growth plate (GP) of the distal femur has a normally curved configuration, and its sides are parallel. The articular cartilage (AC) of the femur and patella are of uniform thickness. (B) Longitudinal section of distal femur and knee from a 4-month-old *sedc/sedc* mouse. The growth plate (GP) of the distal femur is two to three times thicker than the control plate and is irregularly thickened. The articular cartilage (AC) of the femur and patella are irregularly thickened compared with the control. (C) Longitudinal section of distal femur and knee from a 1-year-old *sedc/sedc* mouse. The thickened articular cartilage (AC) of femur and patella are undergoing degeneration. Superficial layers are separating from deeper layers. A cleft (C) is present in the growth plate that is quiescent in this older mouse.

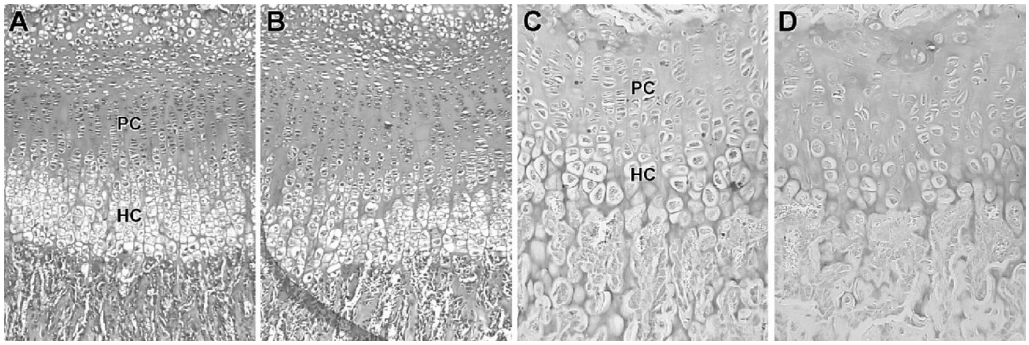

FIG. 6.

(A–D) Midfrontal sections of the proximal growth plate of femurs from (A) a 2-week-old heterozygous control, (B) a 2-week-old with *sedc/sedc*, (C) a 6-week-old heterozygous control, and (D) a 6-week-old *sedc/sedc*. The clear columnar arrangements of the chondrocytes in the proliferative (PC) and hypertrophic (HC) zones of (A and C) controls are nonexistent in (B and D) *sedc/sedc* mice. (Toluidine blue stain: A and B, magnification, ×100; C and D, magnification, ×200).

Table 1

PCR Primers for cDNA Amplification and Sequencing

Designation	Sequence (5′–3′)	Fragment size	Exons
Col2a1f	TGCATGAGGGAGCGGTAGAG	1274	1–16
Col2a1r	TTGGCACCAGGAGCACCAGG		
Col2a2f	TGCTCGGGGTAACGATGGCCAG	1287	16–32
Col2a2r	TCTCCCTTGGGCCCAGCAATG		
Col2a3f	AGGTCTACAGGGAATGCCTGG	1242	32–45
Col2a3r	AATTCTCCTTTGTCACCTCGG		
Col2a4f	GGTGCACAAGGTCCTATGGG	1191	45–52
Col2a4r	GTATCATCAGGTCAGGTCAG		

J Bone Miner Res. Author manuscript; available in PMC 2010 May 4.

Table 2

Measurement of Skeletal Indices

	sedc/+			sedc/sedc		
	***6 weeks* (n = *8*)**	***8 weeks* (n = *7*)**	***16 weeks* (n = *11*)**	***6 weeks* (n = *10*)**	***8 weeks* (n = *8*)**	***16 weeks* (n = *5*)**
Vertebra						
Vertebral height†‡	2.74 ± 0.18	2.99 ± 0.09	3.23 ± 0.14	2.19 ± 0.08**	2.31 ± 0.20**	2.60 ± 0.20**
Vertebral width*†‡	1.93 ± 0.05	1.96 ± 0.07	1.95 ± 0.06	2.14 ± 0.08**	2.38 ± 0.13**	2.35 ± 0.15**
Transverse processes width†	4.80 ± 0.24	5.12 ± 0.25	5.39 ± 0.19	4.75 ± 0.22	5.03 ± 0.41	5.69 ± 0.29
Femora						
Femoral length†‡	14.68 ± 0.24	15.51 ± 0.33	16.45 ± 0.22	12.93 ± 0.32**	13.95 ± 0.64**	14.88 ± 0.41**
Femoral condylar width†‡	3.01 ± 0.05	3.10 ± 0.07	3.16 ± 0.09	3.27 ± 0.13**	3.40 ± 0.12**	3.55 ± 0.16**
Femoral midshaft width†	1.78 ± 0.06	1.78 ± 0.10	1.90 ± 0.12	1.68 ± 0.10	1.76 ± 0.08	1.85 ± 0.11
Tibia						
Tibial length†‡	17.28 ± 0.33	17.80 ± 0.27	18.61 ± 0.24	14.43 ± 0.45**	15.43 ± 0.59**	16.28 ± 0.46**
Tibial condylar width†‡	3.23 ± 0.05	3.27 ± 0.11	3.39 ± 0.11	3.51 ± 0.17**	3.73 ± 0.14**	3.80 ± 0.24**
Tibial midshaft width†‡	1.07 ± 0.05	1.24 ± 0.11	1.16 ± 0.07	1.01 ± 0.05§	1.09 ± 0.04¶	1.08 ± 0.08
Tibial malleolar width†‡	2.42 ± 0.16	2.71 ± 0.24	2.72 ± 0.18	2.68 ± 0.14¶	2.83 ± 0.16	2.92 ± 0.12§

All values are expressed as mean (mm) ± SD.

*Mean width of upper, middle, and lower vertebral width (see Fig. 4).

†Significant effect of time revealed by two-way ANOVA ($p < 0.05$).

‡Significant effect of group revealed by two-way ANOVA ($p < 0.05$).

$^{\S}p < 0.05$

$^{\P}p < 0.01$

$^{**}p < 0.001$ compared with +/nm group of same age (Student's unpaired *t*-test).

Table 3

Bone Histomorphometry of Fifth Lumbar Vertebrae

	+/sedc			sedc/sedc		
	***6 weeks* (n = *8*)**	***8 weeks* (n = *7*)**	***16 weeks* (n = *11*)**	***6 weeks* (n = *10*)**	***8 weeks* (n = *8*)**	***16 weeks* (n = *5*)**
LGR (μm/d)*†	8.96 ± 0.63	7.19 ± 1.34	3.69 ± 0.85	5.62 ± 0.93¶	4.70 ± 0.72§	2.18 ± 0.33§
BV/TV (%)†	19.2 ± 3.7	18.9 ± 2.4	21.2 ± 4.6	16.0 ± 3.1	16.4 ± 3.0	16.8 ± 2.0
Tb.Th (μm)†	36.6 ± 3.9	36.4 ± 2.3	40.2 ± 4.8	30.7 ± 3.5§	30.6 ± 3.4§	34.8 ± 1.8‡
OS/TV (%)*†	0.14 ± 0.07	0.10 ± 0.04	0.06 ± 0.05	0.09 ± 0.06	0.07 ± 0.04	0.04 ± 0.04
MAR (μm/d)*†	1.70 ± 0.23	1.49 ± 0.21	1.39 ± 0.21	1.49 ± 0.25	1.24 ± 0.25	1.19 ± 0.31
BFR/TV (%/y)*†	142.8 ± 26.4	94.2 ± 22.0	76.0 ± 20.4	96.4 ± 46.5‡	74.6 ± 18.3	49.0 ± 17.0‡
ES/BS (%)*	16.1 ± 3.2	12.2 ± 3.3	8.4 ± 2.7	14.2 ± 4.3	11.4 ± 3.7	7.1 ± 3.7
Oc.S/BS (%)*	5.4 ± 1.4	4.6 ± 1.2	3.8 ± 1.2	5.2 ± 1.8	4.5 ± 1.3	2.8 ± 1.3
N.Oc/TV (/mm^2)*†	12.1 ± 8.4	9.7 ± 2.1	6.1 ± 2.4	8.4 ± 3.3‡	6.6 ± 2.8‡	4.1 ± 2.1

All values are expressed as mean ± SD.

*Significant effect of time revealed by two-way ANOVA ($p < 0.05$).

†Significant effect of group revealed by two-way ANOVA ($p < 0.05$).

$^{\ddagger}p < 0.05$

$^{\S}p < 0.01$

$^{\P}p < 0.001$ compared with +/nm group of same age (Student's unpaired *t*-test).